4. DYNAMICS OF A WHEELSET WITHIN A BOGIE FRAME

4.1. INTRODUCTION

Using the inertial reference frame (IRF) modelling platform described in Chapter 3, a computer program for the simulation of the dynamics of wheelsets within a bogie frame is developed and reported in this chapter. The program is named the Rail Bogie Dynamics (RBD) program for convenience. The RBD program is currently developed in MATLAB environment. The limited size of the problem solved as part of this thesis has never posed problems related to computational time; if that becomes a serious issue, the algorithm based on the formulation provided in Chapter 3 could be programmed in alternate languages such as FORTRAN or C++.

First the RBD program has been used to examine the dynamics of railway wheelsets as these are the basic units that provide guidance for the wagon on the track. The wheelset is assembled with the suspension system to provide stability whilst they are at rest and in motion. The assemblages are known as bogies. The bogies of locomotives usually have three wheelsets each, whilst the bogies of the wagons and passenger cars have two wheelsets each. Some utility wagons containing single wheelset bogies are also used in the industry.

Irrespective of the design of the bogie system, the stability of wagons in motion is largely dictated by the dynamics of the wheelset within the bogie frame (Wickens (2003)). Therefore a very simple form of a bogie system containing a single wheelset within a bogie frame is considered for the examination of its dynamics using the RBD program. First the dynamics of this assembly has been investigated under the steadystate (constant speed) condition using the RBD program and the results validated against a commercial software package VAMPIRE (Evans (1999)). Second, the RBD program has been used to simulate the effect of longitudinal braking and traction torques to the dynamics of the simple bogie. This chapter reports the process and results of these analyses.

4.2. DESCRIPTION OF MODELLED SYSTEM

In order to understand the railway wagon dynamics, it is common to investigate the motion of a single wheelset running on the track. However, in actual condition, the wheelset is attached to a bogie frame that restricts its motion. Therefore, in this investigation the wheelset is connected to a mass, which represents the sprung mass of the bogie frame or the wagon body. The connection is formed by a set of linear springs and dampers in the longitudinal, the lateral, and the vertical directions as shown in Fig. 4.1. The lateral distance between the right and the left suspension was 0.7 m. The characteristics of the springs and dampers are presented in Table 4.1. The characteristics of the springs and dampers have been optimized in such a way that the bogie is stable up to 25 m/s (90 km/h). As a reference, the critical speed of wagons containing three-pieces bogies running on the rigid track calculated by Sun (2002) is in the range between 79 km/h – 159 km/h, depending on the wheel profile and wheel radius being used. The inertia properties of the wheelset and the bogie frame used in the simulation are given in Table 4.2. The mass and moment of inertia of the bogie frame is chosen so that the axle load represents the axle load of the common normal operation of four axle wagons.

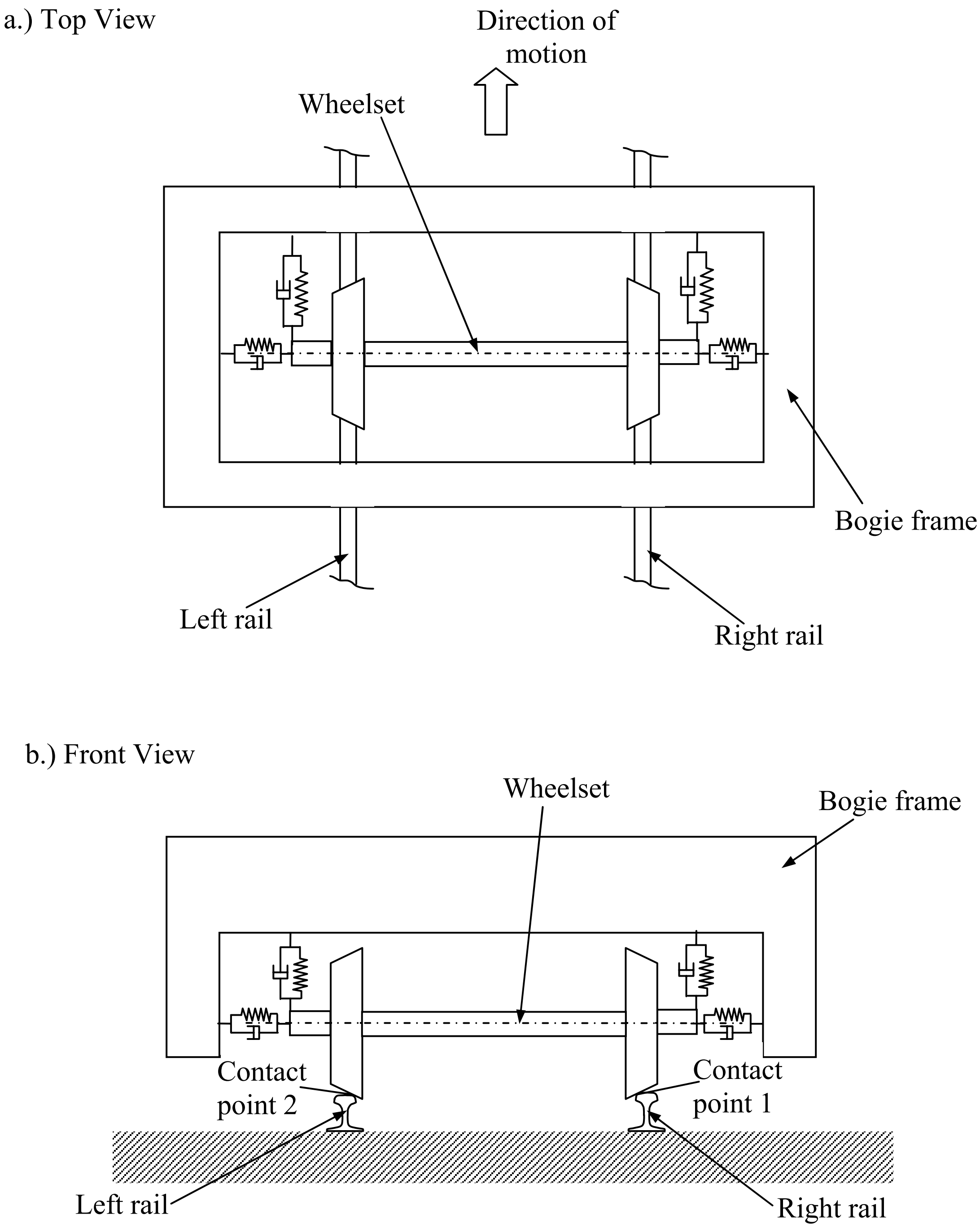

Figure 4.1. A wheelset within a bogie frame

Because the bogie frame is supported only by two vertical springs (on the left and the right), an unbalanced moment with respect to the lateral axis will act on the bogie frame. In anticipation of this, a constraint is added so that the pitch degree of freedom of the bogie frame is eliminated. Therefore the bogie frame is represented with five degrees of freedom only. The springs and dampers are attached to the wheelset at the points on the rotation axis of the axle (lateral axis of wheelset body reference frame). By using such an arrangement the points of connection do not rotate about the axle so the additional revolute joint is not needed.

Table 4.1. Spring and damper characteristics

	Spring Stiffness , K (N/m)	Damping Coefficient, C (N.s/m)
Longitudinal	20×10^4	10×10^3
Lateral	8×10^4	6×10^3
Vertical	5×10^4	4×10^3

Table 4.2. Inertia properties of the wheelset and the sprung mass

	Wheelset	Sprung Mass
Mass (kg)	1200	10000
Mass moment of inertia I_{xx} ($\mathrm{kg \cdot m^2}$)	720	20000
Mass moment of inertia I_{yy} ($\mathrm{kg \cdot m^2}$)	112	15000
Mass moment of inertia I_{zz} ($\mathrm{kg \cdot m^2}$)	720	20000

For generalisation, the left and the right rails are considered as separate bodies constrained to the ground. Thus, the total number of bodies in the system is four (the right rail, the left rail, wheelset and bogie frame). With this assumption it is possible to simulate different lateral and vertical irregularities for each rail and also track gauge widening at the curve where the outer and inner rails each have a different curve radius. In spite of these opportunities, this thesis has neither considered the rail geometry irregularity nor other defects due to its primary focus on the effect of longitudinal forces to wheelset / bogie dynamics.

All the bodies involved are assumed as rigid with the body reference frames attached to their respective centres of mass. The motion of each body's local coordinate system with respect to the global system is described in the multibody formulation using three translational coordinates and four Euler parameters. For the system containing four rigid bodies, the vector of generalised coordinates is written as

$$\mathbf{q} = \begin{bmatrix} \mathbf{q}^{rr} & \mathbf{q}^{rl} & \mathbf{q}^{ws} & \mathbf{q}^{bf} \end{bmatrix}^{\mathrm{T}} \tag{4.1}$$

where $\mathbf{q}^{rr}, \mathbf{q}^{rl}, \mathbf{q}^{ws}, \mathbf{q}^{bf}$ are vectors of generalised coordinates of the right rail, the left rail, the wheelset and the bogie frame respectively. As the vector of the generalised coordinates of each body has seven components (three translational coordinates and four Euler parameters) the total vector coordinates will have a total of 28 components.

The vector of the non-generalised surface parameters is written as

$$\mathbf{s} = \begin{bmatrix} \mathbf{s}_1^{rr} & \mathbf{s}_2^{rl} & \mathbf{s}_1^{ws} & \mathbf{s}_2^{ws} \end{bmatrix}^{\mathrm{T}} \tag{4.2}$$

where each superscript represents a body as described in Eq. (4.1) and the subscript represents the number of each contact point (contact point 1 is located at the right wheel-rail patch and contact point 2 is located at the left wheel-rail patch; see Fig. 4.1). Because each contact surface is represent by two surface parameters, vectors of non-generalised surface parameters in Eq. (4.2) will have eight components. Thus, the vectors of the generalised and the non-generalised coordinates will have 36 components in total.

Inducing four Euler parameter constraints (one for each body), ten contact constraints, twelve ground constraints, and one constraint of the bogie frame pitching, there will be a total of 27 constraint equations and hence there will be nine (36-27=9) unrestrained degrees of freedom. The 27 constraint equations also imply that the size of the sub-Jacobian matrix $\mathbf{C_q}$ is 27×28 and the size of the sub-Jacobian matrix $\mathbf{C_s}$ is 27×8. Hence, the total dimension of the augmented matrix of the mass matrices and sub-Jacobian matrices in Eq. (3.75) is 63×63. For the constant speed simulation a velocity constraint in the longitudinal direction is added, which increases the dimension of the augmented matrix to 64×64 and reduces the unrestrained degrees of freedom to eight.

4.3. WHEEL AND RAIL PROFILES

The wheel and the rail profile used in the simulation are shown in Fig. 4.2. AS 60 kg/m plain carbon rail and LW2 wheel profile in new condition are considered. Both profiles are taken from Queensland Rail (QR) data. The method of formulation of the wheel rail contact in the RBD program demands the derivatives of the spline representation of the wheel and the rail profile up to the third order. Therefore, fifth- order splines have been selected. For this purpose spline curves that represents the wheel and the rail profile are generated from the measured data points by using Spline2 V6.0 software developed by Delft University of Technology (Thijse (2002)).

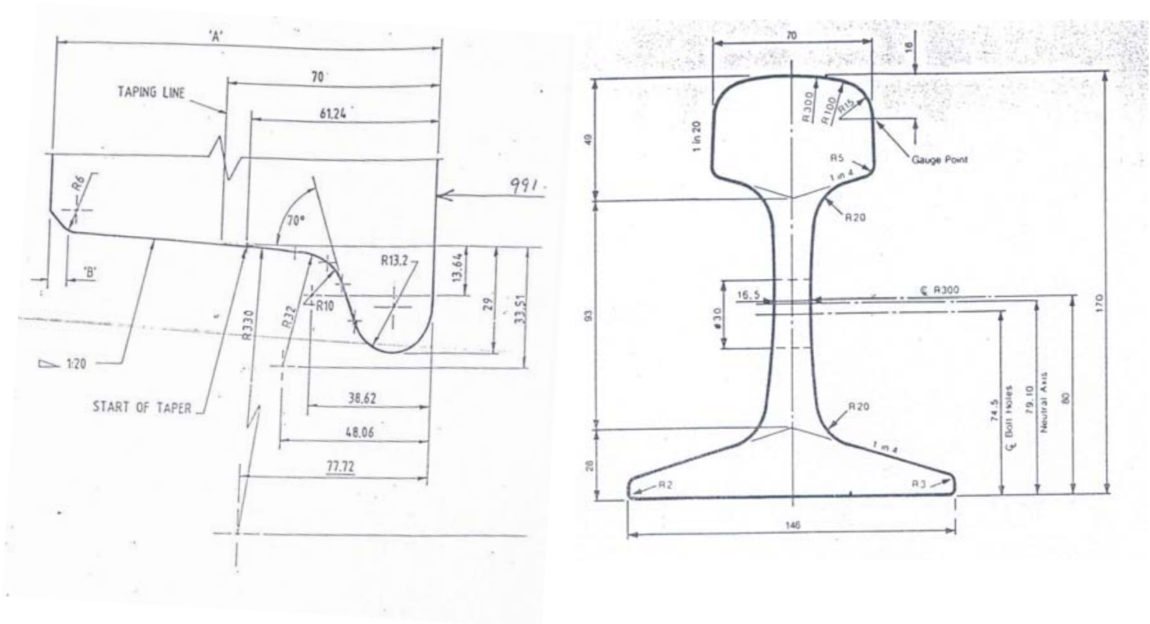

(a) wheel profile (b) rail profile

Figure 4.2. Technical drawing of the wheel and the rail profile

Fig. 4.3 shows the spline representation of the wheel profile which is generated using a fifth-order polynomial. The spline curve covered the profile of the wheel tread up to the flange tip.

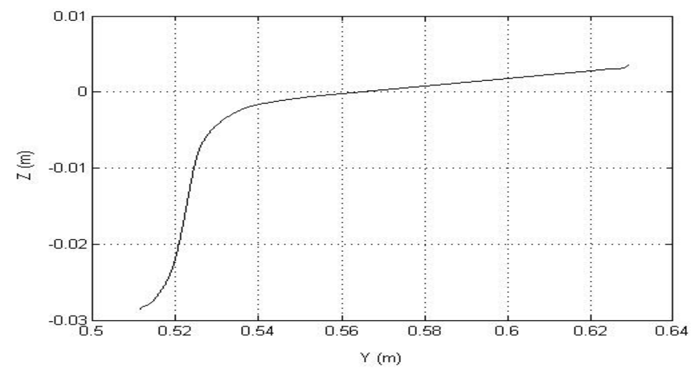

Figure 4.3. Spline curve of the wheel profile

Fig. 4.4 shows the 1st , 2nd , and 3rd derivatives of the wheel profile. From the figures we can see that the smooth (i.e. no point of singularity) and continuous curves are obtained until the third derivatives. Such continuous and smooth curves are required for improving the accuracy and also to avoid numerical instability during the solution phase of the simulation.

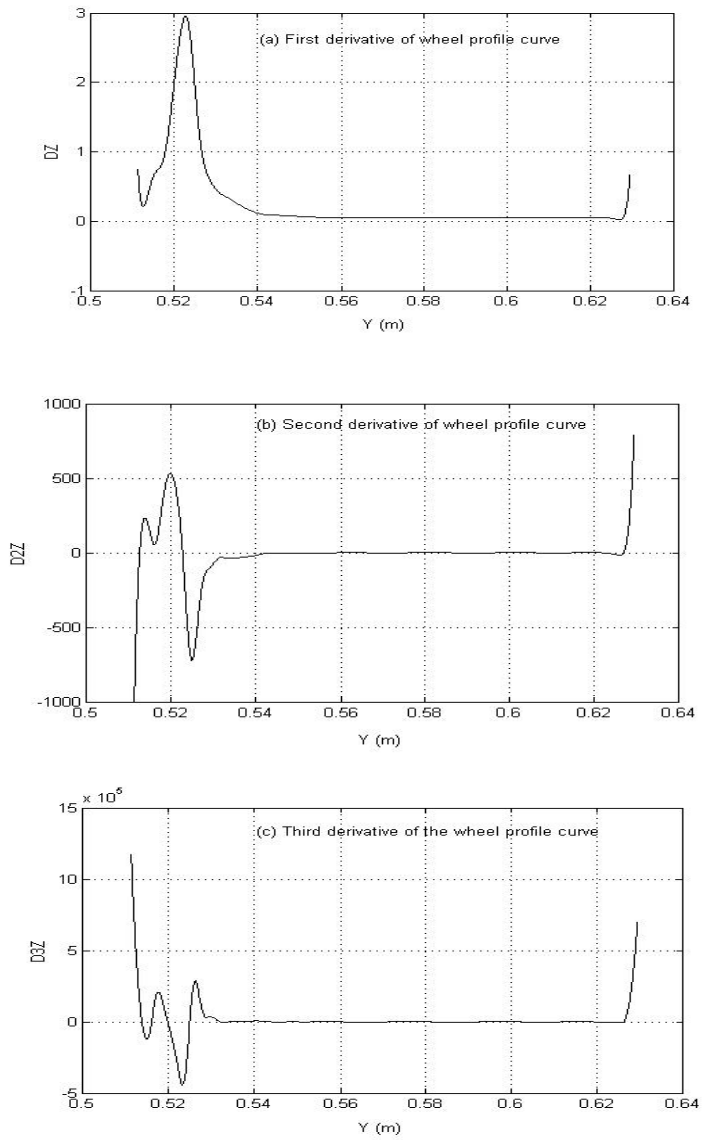

Figure 4.4. Derivatives of the wheel profile curve

Rails are normally fitted to the track containing concrete sleepers with 1 in 20 inclination (Esveld (2001)). Fig. 4.5 shows the spline representation of the rail profile with 1 in 20 inclination and Fig. 4.6 shows its first three derivatives; all function are seen to be continuous and smooth. Similar to the wheel profile spline, the rail profile spline was also generated using a fifth-order polynomial.

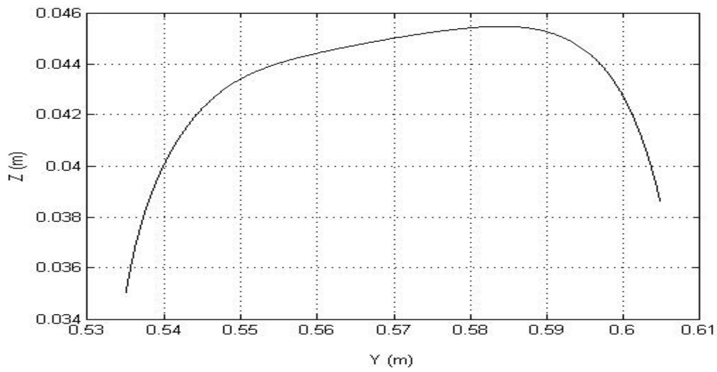

Figure 4.5. Spline curve of the rail profile

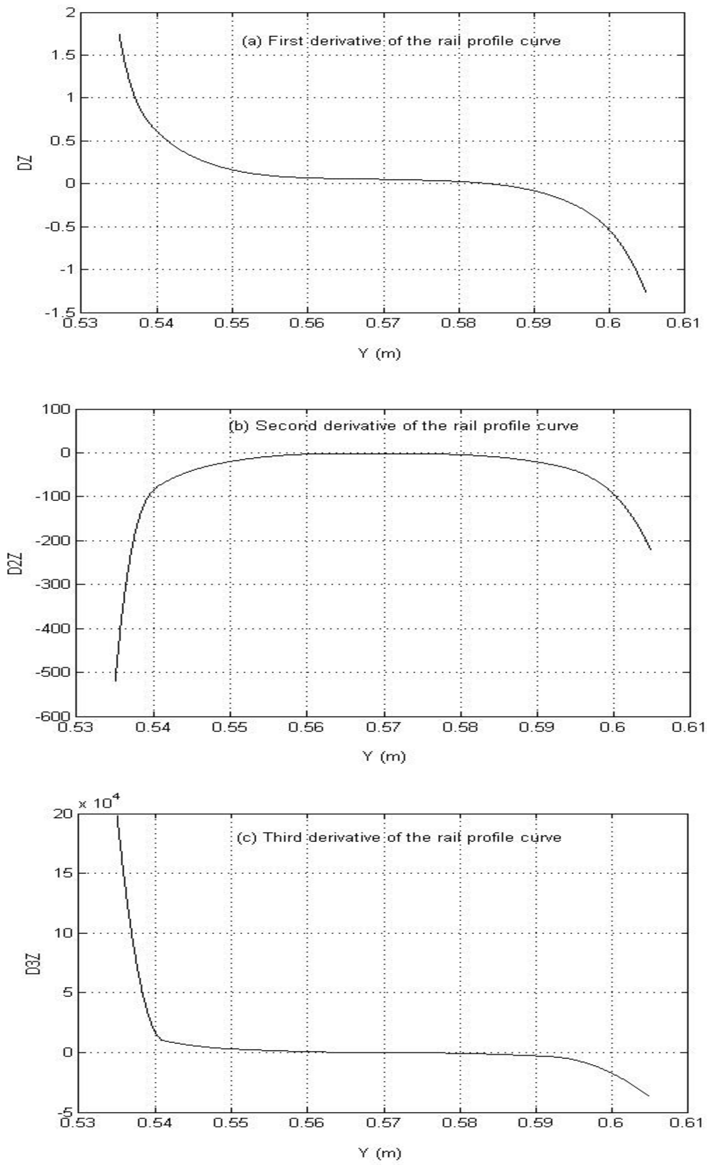

Figure 4.6. Derivatives of the wheel profile curve

Placing the wheelset on the centre of narrow gauge track (1067mm) and applying the law of contact between rigid bodies, the contact point between wheels and rails could be found as shown in Fig. 4.7. The nominal distance between the left and the right contact points was 1140 mm.

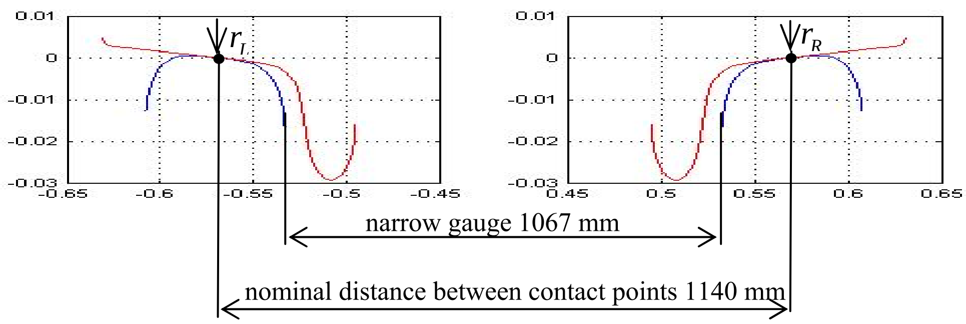

Figure 4.7. Wheelset on narrow gauge track

In the centre position the rolling radius of the right wheel and the left rail are equal ($r_R = r_L = r_w =$ *nominal radius*). Shifting the wheelset to the left and/or to the right causes differences between the rolling radius of the right and the left wheels. The rolling radius difference between the right and the left wheels is the important parameter that defines the wheelset dynamics. This parameter is plotted in Fig. 4.8. The figure reveals that the change of rolling radius difference was linear until flange contact occurred at approximately 9.5 mm lateral shifting of the wheelset.

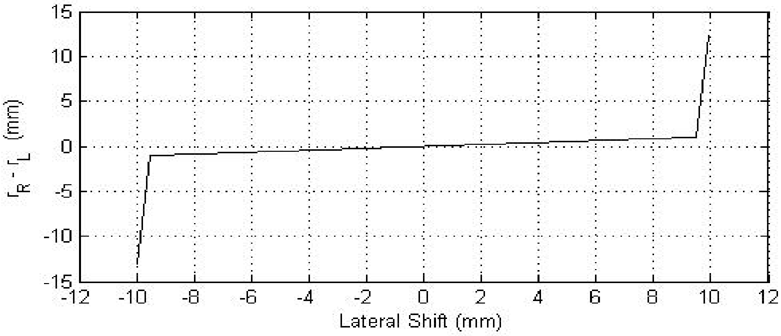

Figure 4.8. Rolling radius difference

4.4. SIMULATION AT CONSTANT SPEED

The results of the simulation using the RBD program are compared with that of VAMPIRE which is used by many railway wagon manufacturers and operators to investigate the dynamics of railway wagons in the design and operational phases (AEA Technology Rail (2004)). VAMPIRE uses the TFR coordinate system that moves at a pre-defined speed along the track and does not explicitly account for the wheelset pitch (AEA Technology Rail (2003)). These are the major difference between VAMPIRE and the RBD program. The other difference is that VAMPIRE calculates all the contact parameters (angle and radius) separately prior to the simulation and interpolates them during simulation, whilst the RBD program calculates these parameters using the contact law algorithm (see Section 3.2.5) in every time step of the simulation.

The cases that were simulated included the system of a wheelset and a bogie frame travelling on a tangent track with specified constant forward velocities. At a specified distance of travel a lateral disturbance in the form of track lateral displacement was provided to the wheelset to initiate lateral oscillation. The coefficient of friction between the wheel and the rail was assumed to be 0.3 in all cases of simulation. To gain a comprehensive view on the results, simulations were carried out with various velocities, starting from the low speed where the wheelset motion remained stable to the high speed where the wheelset motion became unstable. Some important results of the simulation at three selected velocities of 15 m/s, 25 m/s, and 30 m/s are presented in this chapter.

Fig. 4.9 shows the lateral displacement against the travel distance of the wheelset and bogie frame at 15 m/s. The result presented in this figure is obtained using the RBD program. From the figure it can be seen that the wheelset and the bogie frame have had damped lateral oscillations. The decrement of the wheelset oscillation shows a high damping ratio. The oscillations have a 13.25 m wavelength; for the speed of 15 m/s, this wavelength is associated with a frequency of 1.13 Hz. The oscillation of the bogie frame follows the wheelset oscillation with the same wavelength but with almost 180^{o} phase lag due to the existence of the spring and damper system.

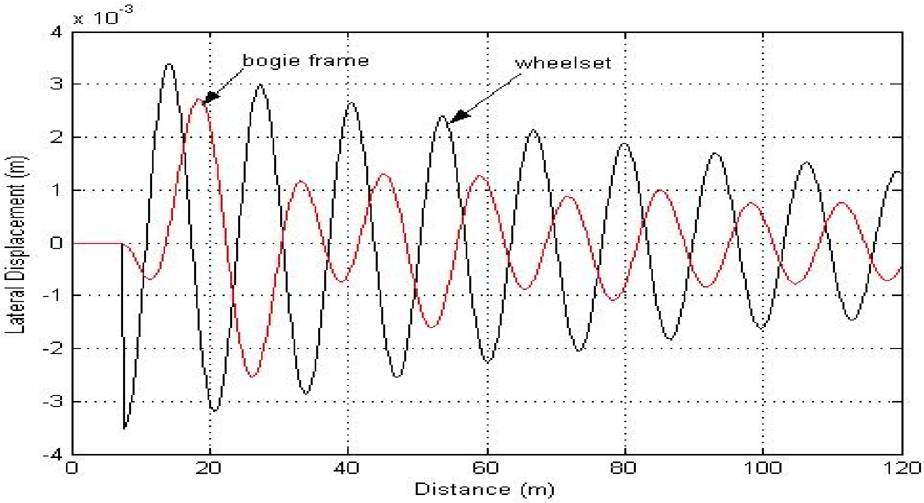

Figure 4.9. Lateral displacements - RBD Program at V=15 m/s

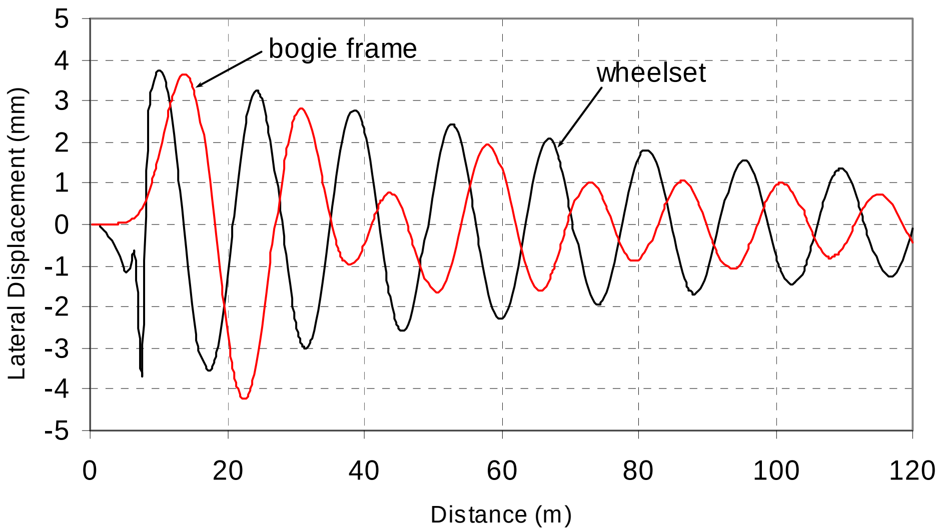

Figure 4.10. Lateral displacement - VAMPIRE at V=15m/s

Fig. 4.10 exhibits the lateral displacement of the wheelset and bogie frame simulated by VAMPIRE for the speed of 15 m/s. This figure shows, in general, the same trend and magnitudes as that provided by the RBD program presented in Fig. 4.9. The oscillation of the bogie frame shows a similar lag of about 180^{o} phase difference compared to the wheelset oscillation. The wheelset and the bogie motions are also damped well. However the wavelength of the oscillation calculated by VAMPIRE is 14 m which is slightly larger than that calculated by the RBD program (13.25 m). For the speed of 15 m/s this wavelength is associated with a frequency of 1.07 Hz (RBD predicted frequency is 1.13 Hz). These results correspond to an error margin of 5.6 %, which is considered negligible given both programs use entirely different formulations. With the nominal radius of 0.425 m and nominal lateral distance between left and right contact points of 1140 mm (Fig. 4.7), by using the simple Klinger formulation in Eq. (2.1) of Chapter 2, the wavelength of 13.25 m resulted from the simulation using RBD program is associated with 0.054 effective conicity, while the wavelength of 14 m calculated by VAMPIRE is associated with the effective conicity of 0.049 (an error margin in conicity of 10.2 % that is considered acceptable).

Fig. 4.11 exhibits the longitudinal and lateral creep forces at the right wheel-rail contact point calculated by the RBD program while Fig. 4.12 exhibits the same information calculated by VAMPIRE, both for the velocity of 15 m/s. From Figs. 4.11 and 4.12 we can clearly see that the values of the longitudinal creep forces obtained from both simulations agree very well. The RBD program and VAMPIRE calculate the longitudinal creep force that oscillates around zero with the maximum amplitude of about 0.2 kN. However, the value of the lateral creep forces calculated by the RBD program is approximately 8.4% larger than the value calculated by VAMPIRE. The

RBD program uses Polach's formulation to calculate the creep forces while VAMPIRE uses look-up tables generated from Kalker exact theory. A small variation in creep forces is thus considered acceptable.

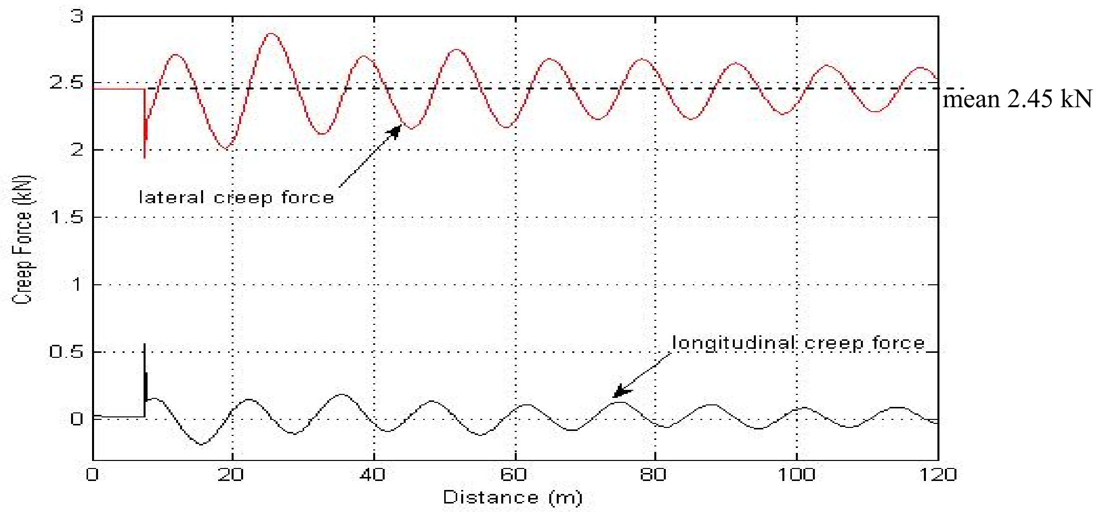

Figure 4.11. Creep forces at the right W/R contact point -RBD Program at V=15 m/s

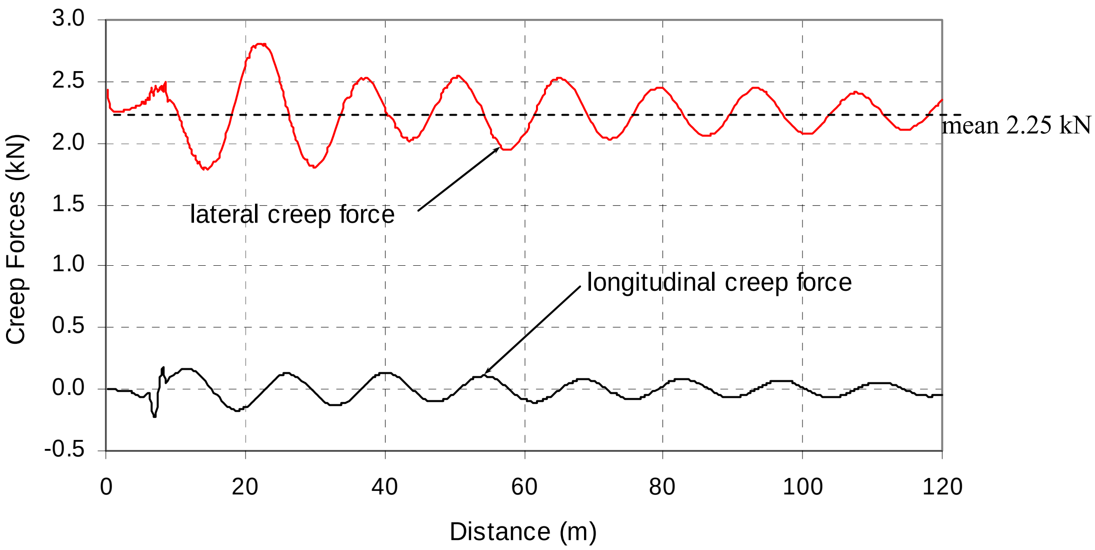

Figure 4.12. Creep forces at the W/R right contact point - VAMPIRE at V=15m/s

Fig. 4.13 and Fig. 4.14 show the lateral displacements calculated for the speed of 25 m/s by using the RBD program and VAMPIRE respectively. Both figures agree very well and the system is still found to be stable. Compared to the simulation for the 15 m/s, however, the oscillations exhibit lower damping. The wavelengths do not change as they only depend on the wheel and the rail profile used. As a consequence, the associated oscillation frequencies become larger due to higher speed. For the simulation using the RBD program the oscillation frequency now becomes 1.89 Hz and for the simulation using VAMPIRE it now becomes 1.79 Hz (an error margin of only 5 %).

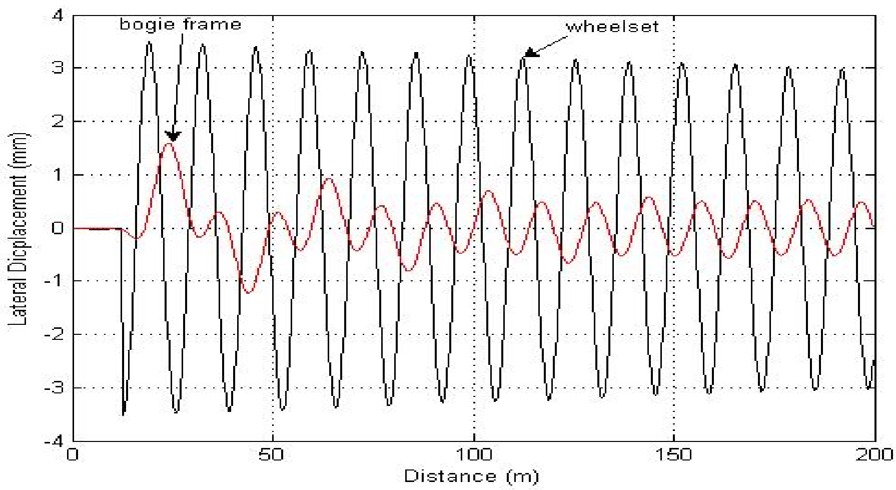

Figure 4.13. Lateral displacements - RBD Program at V=25 m/s

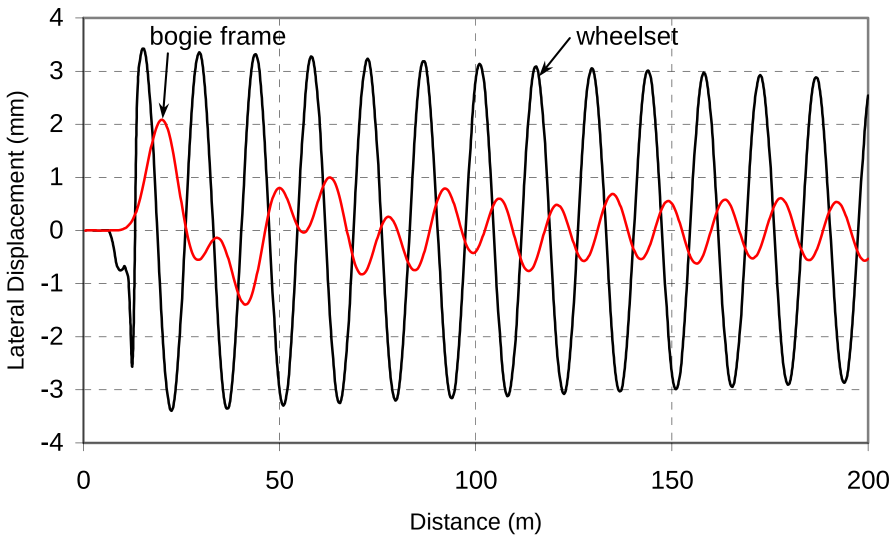

Figure 4.14. Lateral displacement - VAMPIRE at V=25m/s

The creep forces resulted from the simulation for 25 m/s using the RBD program and VAMPIRE are shown by Fig. 4.15 and Fig. 4.16 respectively. There are relatively no significant differences in values in comparison to the creep forces calculated in the simulation for the velocity of 15 m/s. In general, the results calculated by both programs present very good agreement.

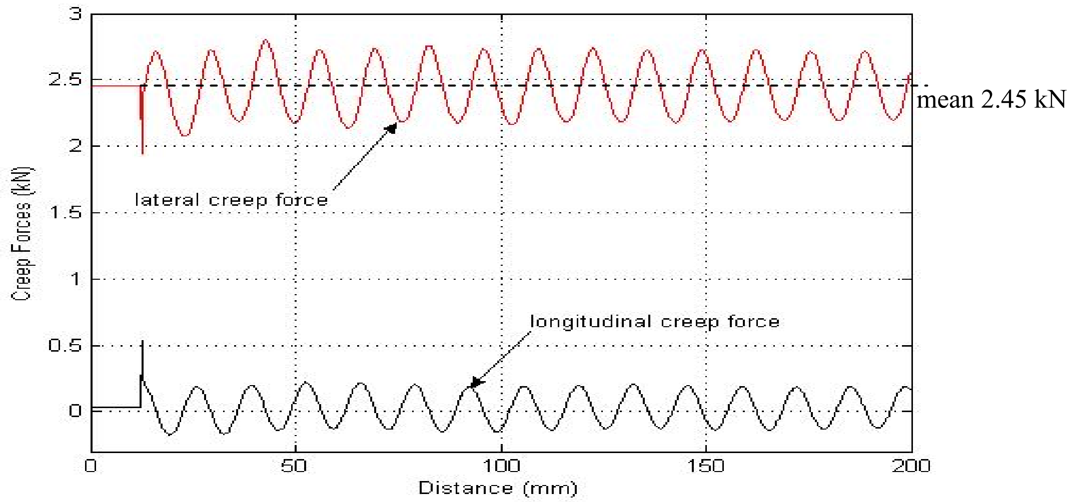

Figure 4.15. Creep forces at the right W/R contact point - RBD program at V=25 m/s

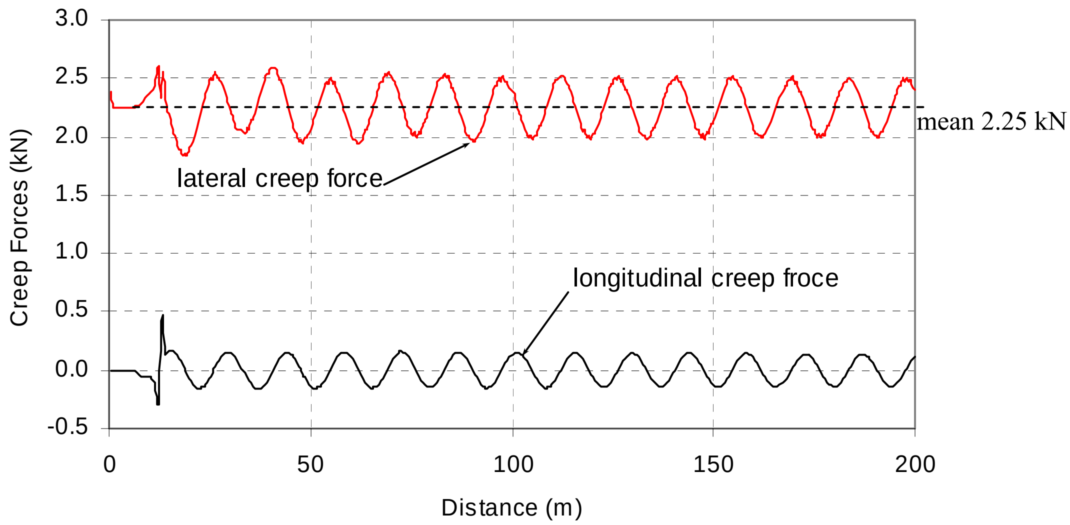

Figure 4.16. Creep forces at the right W/R contact point - VAMPIRE at V=25 m/s

For the velocity of 30 m/s, the simulation using both the RBD program and VAMPIRE show that the system becomes unstable as exhibited in Fig. 4.17 and Fig. 4.18. Further refined simulations using the RBD program and VAMPIRE have shown that the system actually just begins to exhibit unstable response at a velocity of approximately 27 m/s.

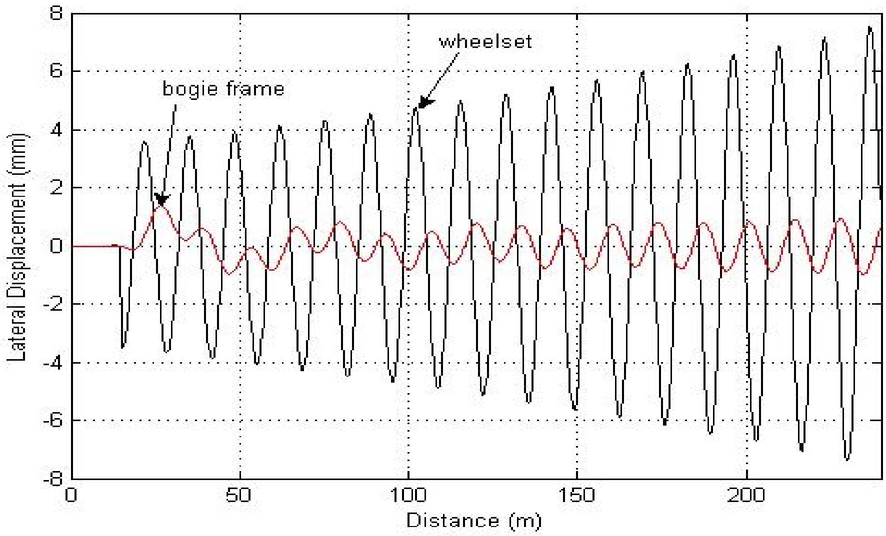

Figure 4.17. Lateral displacements calculated by RBD program at V=30 m/s

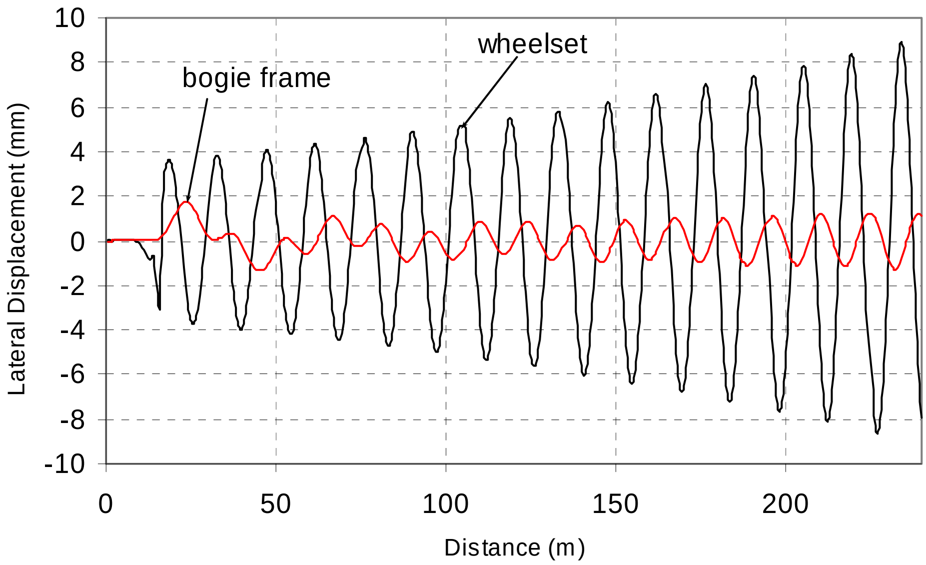

Figure 4.18. Lateral displacements calculated by VAMPIRE at V=30 m/s

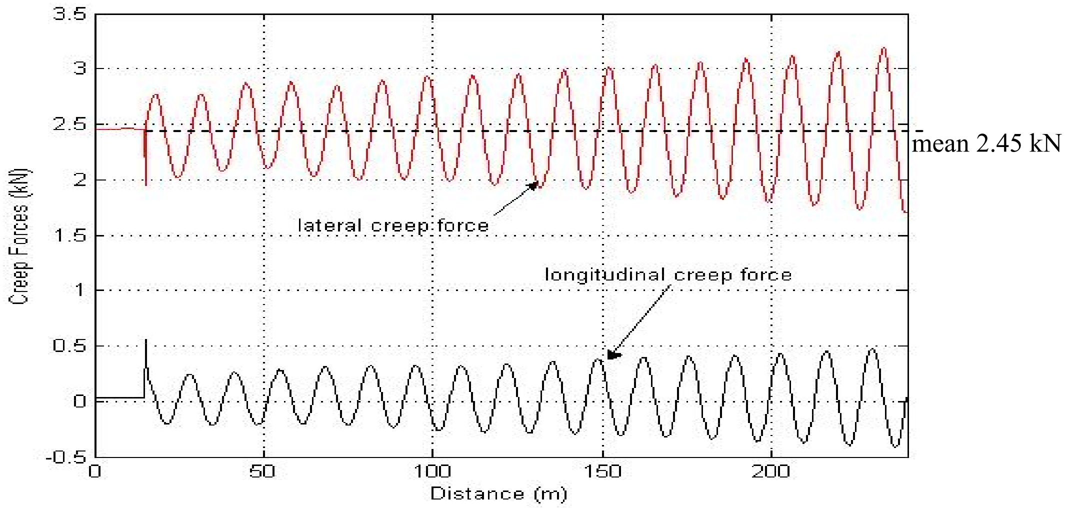

Figure 4.19. Creep forces at the right W/R contact point - RBD Program at V=30 m/s

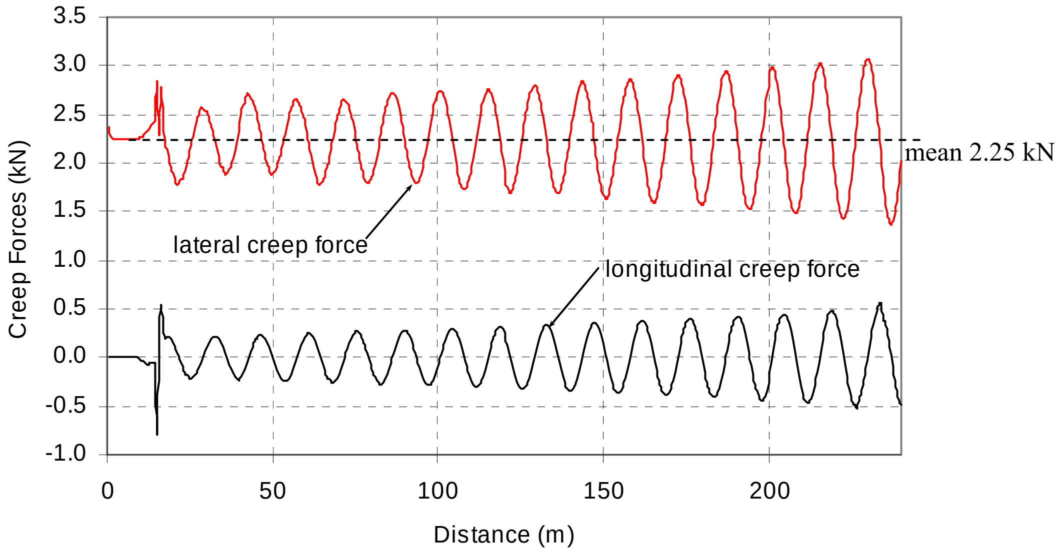

Figure 4.20. Creep forces at the right W/R contact point - VAMPIRE at V=30 m/s

The creep forces at the velocity of 30 m/s calculated by the RBD program is presented in Fig. 4.19 while Fig. 4.20 presents the calculated creep forces using VAMPIRE for the same velocity. Like the simulation at the lower speeds, both results show very good agreement. Compared to the creep forces calculated at the speeds where the wheelset motion is stable, the creep forces calculated at the speed of 30 m/s show a different trend where they increase following the unstable motion of the wheelset.

In conclusion, the results obtained from the constant velocity simulation using the RBD program compare very well with the results provided by VAMPIRE. The insignificant differences on the calculated wavelengths, frequencies and the lateral creep forces indicate that the RBD program, although formulated using a fundamentally different coordinate system, is capable of reproducing the results of the VAMPIRE simulation. From the constant velocity simulation results presented in this section, we could conclude that the IRF system formulation presented in Chapter 3 and the RBD program developed based on the formulation are appropriate for general analysis of the dynamics of wheelsets contained within a bogie frame.

4.5. SPEED PROFILE - EFFECT OF LONGITUDINAL FORCES

In the modelling using the track-following reference (TFR) platform, the speed of wagons is an input that is also used to define the velocity of the reference frame. To do the simulation under variable speed with this method of modelling, a speed profile has to be predefined. However, in real-life conditions, speed change is caused by the application of longitudinal forces either due to braking or traction. In other words, the speed profile is a dependent variable that is affected by the independent action of longitudinal forces. Therefore, to closely simulate the real-life conditions, these longitudinal forces must be input into the simulation models and the speed profile must be output from the simulation model. Unfortunately simulation models based on the TFR formulation (for example VAMPIRE) can not perform the task in this manner.

The RBD program is capable of performing this task that reflects the real-life situation adequately as described in Chapter 3.

To illustrate the capability of the RBD program in producing the speed profile as an output of the simulation, the system of wheelset and bogie frame considered in Section 4.4 was subjected to traction and braking torque sequences provided in Fig. 4.21. The simulation commenced with the initial speed of 10 m/s.

The application of the traction and the braking torque modified the velocity of the system in the longitudinal direction. This is shown in the output of the simulation in Fig. 4.22 (a). The figure shows that the longitudinal velocity of the bogie increases from 10 m/s to 25 m/s in about 15 seconds, which means an acceleration of about 1 m/s^2. With the total mass of the wheelset and bogie frame of 11200 kg, a simple calculation can determine that the 5000 N.m traction torque applied to the wheel that has a radius of 0.425 m will accelerate the system at the rate of 1.05 m/s^2. The acceleration obtained from the simulation is approximately 5% smaller than this value due to the frictional loss at the wheel rail contact patch that occurs in the form of longitudinal creepage or slip. A similar mechanism also occurs during the application of braking torque.

Fig. 4.22 (b) shows the wheelset angular velocity as a function of time, which follows the same trend of the longitudinal velocity. At the maximum longitudinal velocity, the wheelset angular velocity had a value of about 58 rad/s.

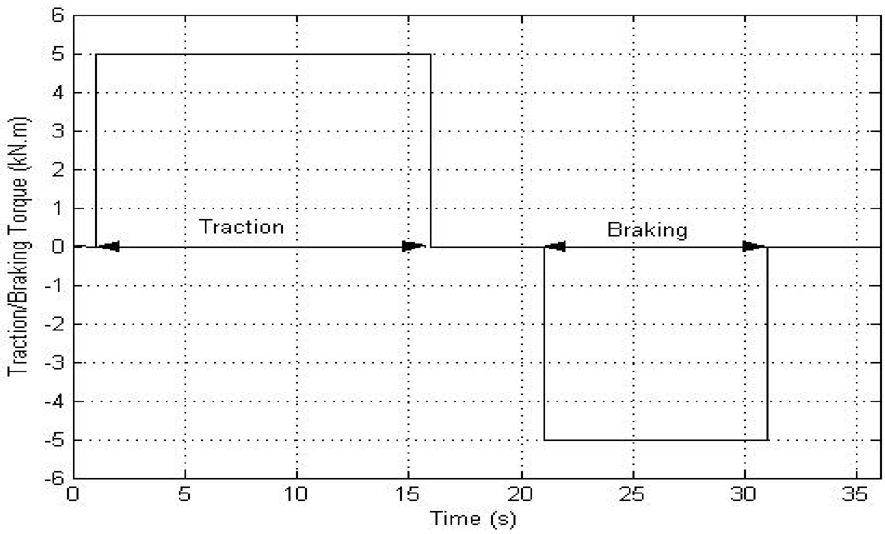

Figure 4.21. Traction/Braking Torque Profile

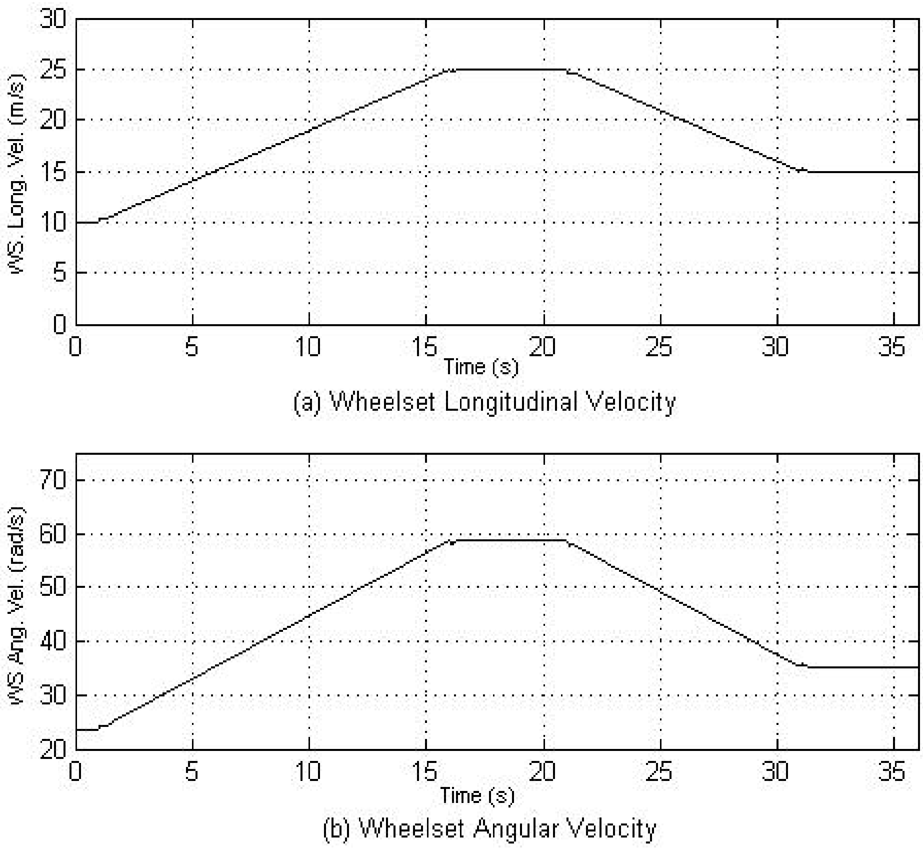

Figure 4.22. Speed Profile

One of the capabilities of the RBD program is the inclusion of the large displacement in the longitudinal direction due to the speed of the vehicle as well as the rotation of the wheelset. This capability is exhibited in the output of the simulation shown in Fig. 4.23. The travel distance of the wheelset as a function of time is presented in Fig. 4.23 (a), while Fig. 4.23 (b) shows the wheelset rotation angle. Both figures show similar trends.

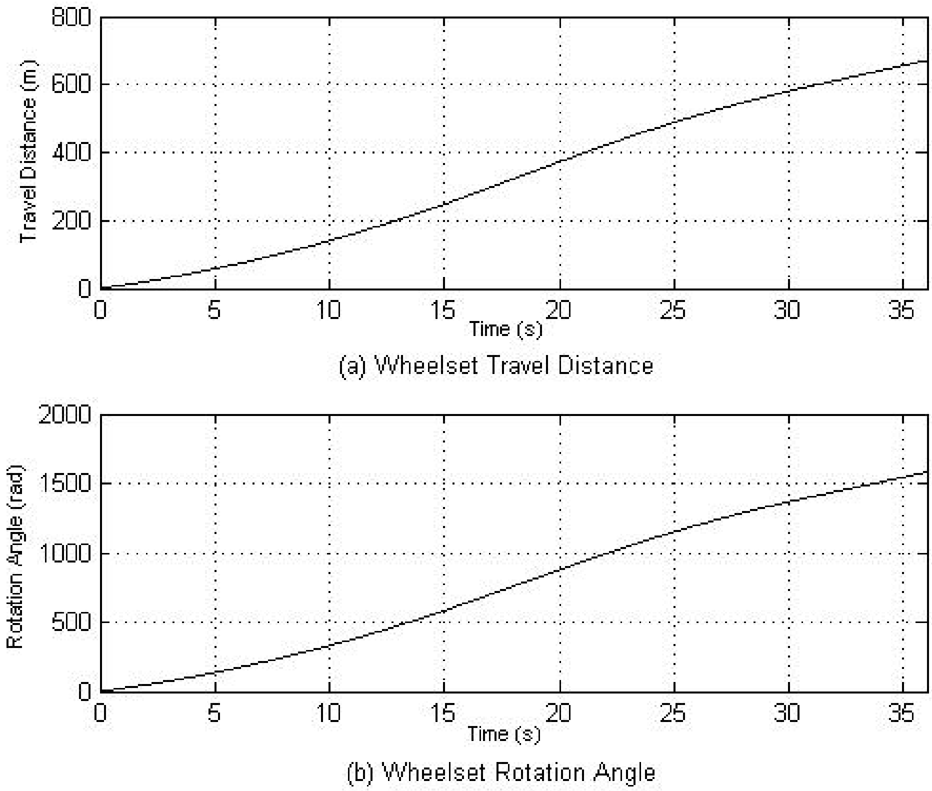

Figure 4.23. Travel distance and wheelset rotation

There are advantages of knowing the total wheelset rotation angle. For example, we can calculate how many rotations are made by the wheelset during travelling a certain distance where the brake or tractive forces are applied. Multiplying the number of rotations with the nominal circumference of the wheel and by comparing the result with the actual travel distance, we can calculate the average slip percentage between the wheel and the rail along the travelling distance. To illustrate this in the present simulation, during the braking ($21 \le t < 31$) the wheelset has made 74.72 rotations (469.52 rad). Without slip this amount of rotation of the wheelset of 0.425 m radius corresponds to 199.55 m of travelling distance. However due to slip the actual distance travelled was 199.65 m that is 0.10 m more. In other words 0.1 m slip travel has occurred during the 199.65 m nominal simulation.

Such outputs of the RBD program shown in this section must be validated. Unfortunately, no tools are found for the purpose. Therefore a laboratory test presenting the bogie under braking condition was performed as part of this thesis. The construction and the results of the testing as well as their comparison with the simulation using the RBD program are reported in Chapter 6 of this thesis.

4.6. LATERAL DYNAMICS UNDER VARIABLE SPEED

The RBD program, similar to other wagon dynamics programs, can predict lateral dynamics of the bogie system due to lateral disturbance. To show this capability, a lateral disturbance was given to the wheelset while it oscillated under the brake or traction force. Fig. 4.24 shows the result of such simulation under braking condition.

As shown in the Fig. 4.24, the simulation started at the speed of 32 m/s. From the simulation at constant speed discussed in Section 4.4, we know that at this speed the oscillation of the wheelset is unstable. The brake force was applied at t = 2.5 sec, as can be seen in Fig. 4.24 (a), where the velocity begin to decrease at that time. Fig. 4.24 (b) shows the associated lateral displacement of the wheelset.

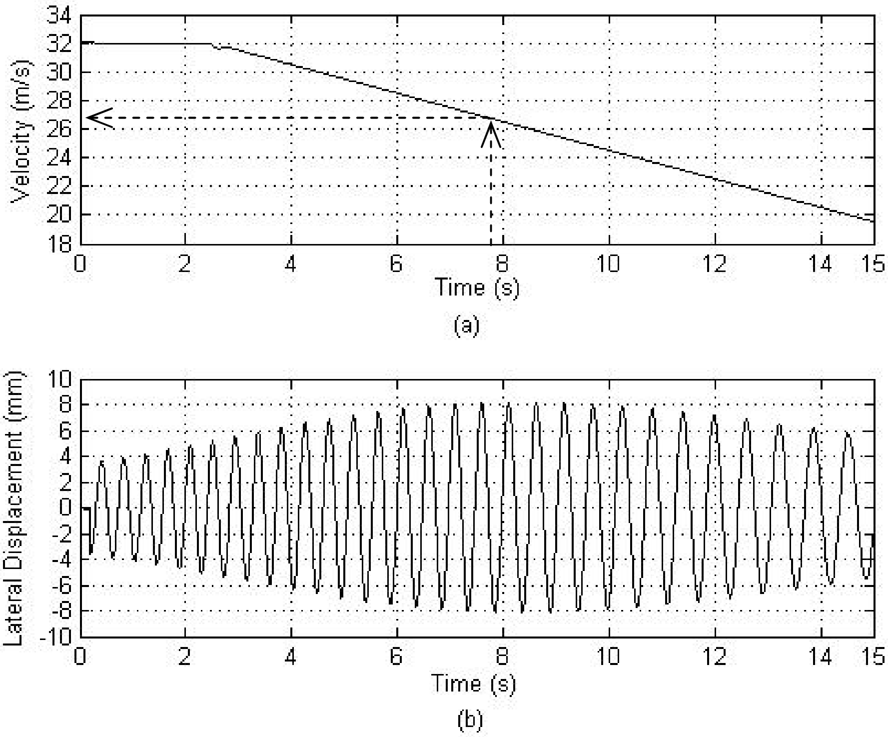

Figure 4.24. Speed profile and wheelset lateral displacement under braking calculated by the RBD program

From these figures it can be seen that the wheelset oscillation remains unstable until the velocity decreases to around 27 m/s; below this speed the oscillation of the wheelset is decayed. Fig. 4.24 (b) also reveals that the frequency of oscillation decreases with the reduction in the velocity. It can be explained that the oscillation wavelength remains constant as it depends only on the wheel and the rail profile. In other words, lower speed provides lower oscillation frequency and higher speed provides higher oscillation frequency.

Utilising the output speed profile of the RBD program shown in Fig. 4.24 (a) as an input, the simulation under variable speed was carried out in VAMPIRE for comparison (as previously explained, in VAMPIRE the speed profile is required as an input). The result of the lateral displacement calculated by VAMPIRE is shown in Fig.

4.25, the value of which closely relates to the lateral displacement calculated by the RBD program.

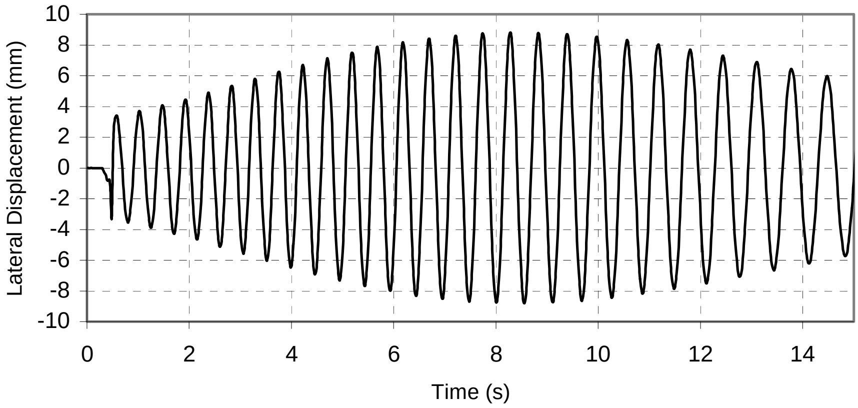

Figure 4.25. Wheelset lateral displacement during braking calculated by VAMPIRE

A similar type of simulation was performed under traction force. The lateral disturbance was given to the wheelset and while it was oscillating the traction force was applied. The result of such simulation is presented in Fig. 4.26. The simulation started at the speed of 20 m/s. At t = 2.5 sec the traction force provided positive torque to the wheelset that increased the speed (Fig. 4.26 (a)). The oscillation of the wheelset was stable until the speed of around 27 m/s (Fig. 4.24 (b)). At speeds higher than this (for example 28 m/s) the oscillation became unstable.

Similar to the simulation under braking condition the output speed profile calculated by the RBD program shown in Fig. 4.26 (a) was used as an input to do the equivalent simulation in VAMPIRE. The associated lateral displacement calculated by VAMPIRE is exhibited in Fig. 4.27.

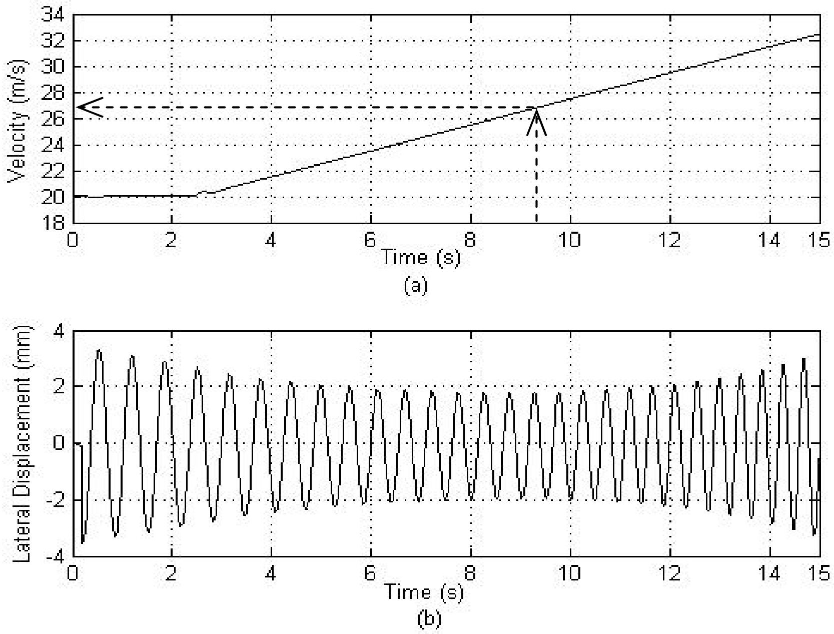

Figure 4.26. Speed profile and wheelset lateral displacement during traction calculated by the RBD program

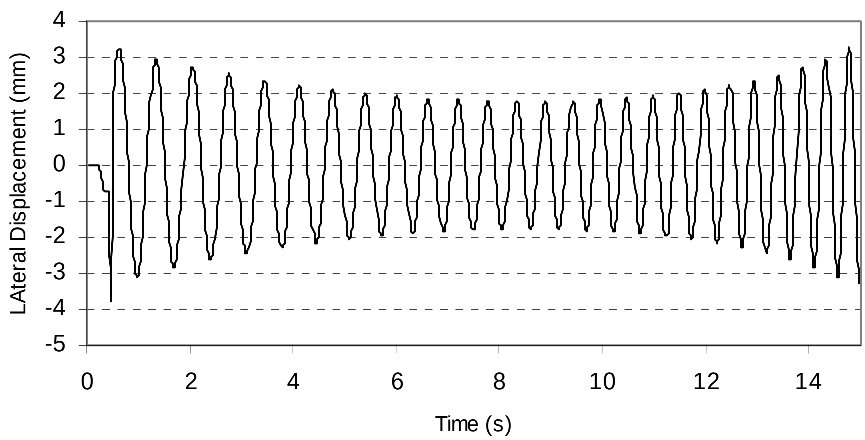

Figure 4.27. Wheelset lateral displacement during traction calculated by VAMPIRE

The above two simulations under variable speed (traction and braking) show that the RBD program can naturally model the effect of the longitudinal force on the longitudinal and the lateral dynamics of the wheelset, whilst VAMPIRE requires precalculated speed profile as an input. The critical speed can also be predicted effectively using the RBD program.

4.7. WHEELSET DYNAMICS UNDER HEAVY BRAKING

When the applied brake force is greater than the available adhesion between the wheel and the rail, skidding occurs. In such condition the wheelset is "locked", i.e. does not rotate, while the body is still in motion. The RBD program has the capability to model such conditions as reported in this section.

A large brake torque (25 kN.m) was applied to the wheelset. Constant friction coefficient between the wheel and the rail is set to be 0.3. With this friction coefficient, and the total mass of the system of 11200 kg, the maximum longitudinal force that can be generated will be around 16.48 kN at each rail. At the nominal wheel radius of 0.425 m, the maximum brake torque that may be applied to the wheelset without causing slip will be around 14 kN.m only.

The simulation started at the speed of 25 m/s as shown in Fig. 4.28 (a) where the motion of the wheelset was still in the stable range. Brake torque was applied at t = 2 sec. From Fig. 4.28 (b) it can be seen that the wheelset rotation has quickly decreased to zero in about 1 sec while the speed was still more than 20 m/s. This means that the wheel has stopped rotating while it still moves forward at high velocity (skid). Fig. 4.28 (c) shows the lateral displacement of the wheelset, indicating very clearly that at the time the skid happens, the motion of the wheelset becomes unstable with very low frequency of oscillation.

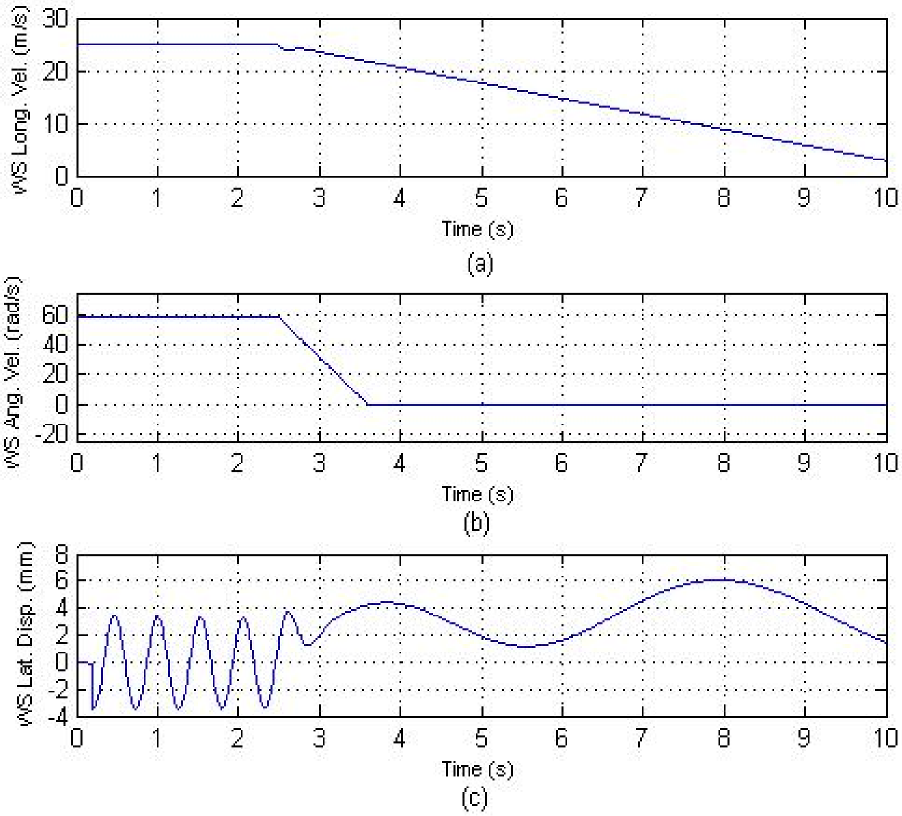

Figure 4.28. Skid at wheel-rail friction coefficient $\mu_r = 0.3$

Fig. 4.29 shows the similar type of simulation with the same brake torque but lower friction coefficient ($\mu = 0.1$) between the wheel and the rail. The situation is more dangerous compared to higher friction coefficient. The reduction in the wheel angular velocity to zero in less than a half second occurred as shown in Fig. 4.29 (b). The wheelset lateral motion is badly unstable, where it has continuously increased without oscillation, as shown in Fig. 4.29 (c).

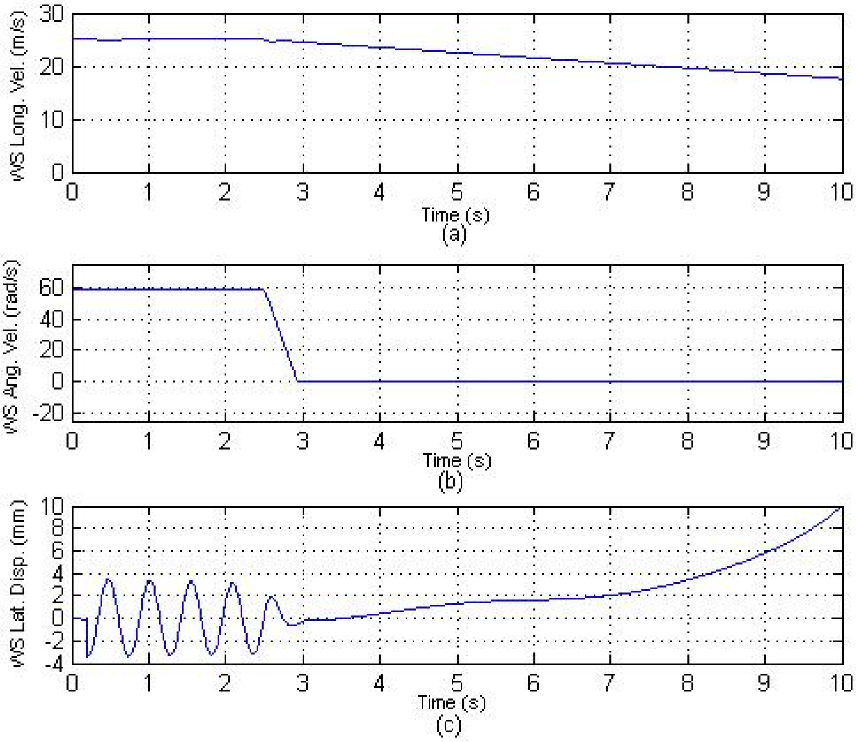

Figure 4.29. Skid at wheel rail friction coefficient $\mu = 0.1$

Both examples of simulation of the skid condition shows the capability of the RBD program to simulate extreme conditions of braking which can not be performed using the software developed using a track-following reference (TFR) platform.

4.8. SUMMARY AND CONCLUSION

This chapter has described the capability of the RBD program in predicting the dynamics of a wheelset within a bogie frame both under constant speed and under variable speed due to traction and braking. Novel features of the RBD program to evaluate the speed profile as a function of input braking / traction torques as well as precisely determining wheelset angular velocity have been demonstrated through examples in this chapter. The results have been validated wherever possible with the simulations using VAMPIRE that illustrated very good agreement. From the results we can draw the following conclusions:

- Under constant speed the wheelset remained laterally stable up to 27 m/s. The insignificant difference between the results of RBD and VAMPIRE might have resulted from the different methods used in the calculation of the contact parameters and creep forces as well as the method of numerical integration used.

- The RBD program can calculate the longitudinal dynamics of the bogie due to the application of traction and braking where the speed profile is an output of the simulation in a natural manner.

- The application of very large braking torques can lead to wheelset skid and tends to destabilise wheelset lateral oscillation. Simulation results showed that skid at the low wheel-rail friction coefficient is more dangerous than at the higher friction coefficient.

- Part of the results of the RBD program, namely the speed profile and skid as a function of the application of brake torque, could only be validated using carefully designed experiments as other commercial dynamics packages do not explicitly account for these factors.